Iranian Journal of Materials Forming 13 (4) (2026) 34-47

IJMF

Online ISSN: 2383-0042

Iranian Journal of Materials Forming

Journal Homepage: http://ijmf.shirazu.ac.ir

Research Article

Evaluation of Residual Stress Relief in a Variable Magnetic Field Using the Nanoindentation Method

Poorya Mardookh Rohani, Sirwan Farhadi* and Arman Hasani

Department of Mechanical Engineering, Faculty of Engineering, University of Kurdistan, Sanandaj, Iran, 15175-66177

ARTICLE INFO

Article history:

Received: 13 February 2026
Reviewed: 7 March 2026
Revised: 18 May 2026
Accepted: 23 May 2026

Keywords:

Residual stress
Electromagnetic stress relief
Nanoindentation

Please cite this article as:

Mardookh Rohani, P., Farhadi, S., & Hasani, A. (2026). Evaluation of residual stress relief in a variable magnetic field using the nanoindentation method. *Iranian Journal of Materials Forming*, *13*(4), 34-47. https://doi.org/10.22099/IJMF.2026.55666.1373

ABSTRACT

Residual stresses can distort mechanical parts and shorten their lifespan. While heat treatment is a common method for stress reduction, limitations such as furnace size and processing time can make it impractical in some cases. Magnetic stress relief offers an alternative approach. This research investigates the relief of residual stress induced by laser welding in 430 steel using the alternating magnetic stress relief method. Applying excitation frequencies near the component's natural frequencies improves the effectiveness of stress relief. Four steel strips were laser-cut to size, annealed, and then laser-welded. Three of the welded strips underwent alternating magnetic stress relief, while the fourth served as an untreated control. All samples were then sectioned via wire cutting at identical distances from the weld line. Nanoindentation was performed on each sample to estimate the residual stress before and after magnetic treatment. Analyzing the force-displacement curves from the nanoindentation test reveals that the alternating magnetic field method significantly reduces residual stresses. The reduction ranges from 38% near the weld line to 84% in the far-field areas. The results demonstrate that high-frequency magnetic stress relief effectively reduces residual stresses despite utilizing relatively simple and inexpensive equipment. While the method demonstrates significant stress reduction, the study is limited to a single material (430 steel) and a specific specimen geometry. Validation through complementary measurement techniques is recommended for future work.

1. Introduction

Residual stresses are an unavoidable consequence of most manufacturing processes involving non-uniform plastic deformation, with welding being a primary source. These locked-in stresses can significantly compromise structural integrity by promoting distortion, reducing fatigue life, and accelerating stress corrosion cracking. Effective stress relief is therefore essential for ensuring the reliability and longevity of welded structures.

Welding is one of the most important production processes and a widely used method of connecting parts.

* Corresponding author
E-mail address: s.farhadi@uok.ac.ir (S. Farhadi)
https://doi.org/10.22099/IJMF.2026.55666.1373

Today, welding is used in many fields such as construction, plumbing, shipbuilding, aerospace, automobile manufacturing, agricultural equipment, household appliances, and construction equipment. Welding is a process that involves local heat generation from a moving heat source. Welded structures are rapidly heated to the melting temperature, followed by rapid cooling. This process changes the microstructure and properties of the material and creates residual stresses [1]. These residual stresses can cause part distortion and significantly shorten component lifespan by contributing to crack initiation and propagation, fatigue failure, and stress corrosion cracking [2]. Therefore, stress-relief methods are suggested to maintain the shape of the parts and increase their strength and life.

Traditional stress relief methods are classified into thermal and mechanical techniques [3, 4]. Thermal methods include pre- and post-heating, while mechanical methods include pinning, static stress, and vibrational stress reduction [3]. Heat treatment is a common method of stress reduction in the metal-forming industry. While this method reduces residual stress, it also has several disadvantages, such as a long processing time, significant energy consumption, the formation of oxide deposits on the surface, and significant effects on the mechanical properties. In contrast, mechanical methods like vibratory stress relief (VSR) offer advantages such as lower energy requirements, shorter treatment durations, and minimal distortion or surface degradation [5].

An emerging alternative is magnetic stress relief, where an external magnetic field induces volumetric forces and controlled heating in metallic components. This method combines the benefits of thermal and mechanical treatments while minimizing their limitations. Magnetic stress relief techniques can be categorized into pulsed and alternating electromagnetic induction methods. The pulsed method employs a high-intensity magnetic field in short bursts, requiring specialized (and often costly) equipment. The alternating field method uses an oscillating magnetic field to induce cyclic stresses within the material. This approach can also generate mild heating, further aiding stress relaxation. In the alternating field method, the excitation frequency, vibration characteristics, and natural frequencies of the workpiece play a key role in the level of induced stresses and how they are distributed. In this method, the input energy increases the movement of dislocation and ultimately leads to the uniform distribution of micro-plastic strain, the release of stored elastic energy, and ultimately the reduction of residual stress [6]. Studies have explored practical applications of magnetic treatment, showing potential for increased service performance and life of components [7].

Residual-stress relief by magnetic treatment has been investigated through several approaches. Among them, the pulsed magnetic method has been studied more extensively than other magnetic techniques and has demonstrated effective residual-stress reduction in a variety of metals and alloys, often without altering the microstructure or mechanical properties [8–20]. Its main advantages include rapid processing, low energy consumption, non-thermal operation, and environmental friendliness. In comparison, alternating magnetic methods and hybrid magnetic treatments remain less explored, although they have shown promising results as alternative stress-relief strategies.

Low-frequency alternating magnetic treatment (typically <100 Hz) has been reported to reduce residual stress in low-alloy steels, with reductions often in the range of 20% to 30% or more [21–24]. This effect is commonly attributed to magnetoplastic deformation, whereby the applied magnetic field interacts with magnetic domains and promotes microscopic plastic deformation, leading to stress relaxation. Prior works on low-frequency alternating field methods demonstrated stress relief at low frequencies. However, these approaches require high magnetic field strengths to induce sufficient dislocation motion, necessitating large, high-power equipment. Additionally, these approaches do not effectively couple with the dynamic response of the workpiece.

Hybrid techniques have also attracted attention because they combine multiple driving forces to enhance dislocation motion. Magnetic-vibration stress relief, for instance, has shown particularly strong performance: the simultaneous application of magnetic excitation and mechanical vibration promotes greater plastic deformation than either treatment alone. Huang et al. [25] compared magnetic-vibration stress relief with single vibration treatment, single magnetic treatment, and sequential combinations of the two. Using an 80 Hz magnetic field together with vibratory excitation, they reported reductions of approximately 39% in transverse residual stress and 55% in longitudinal residual stress for the hybrid method, compared with roughly 19–20% for single vibration treatment and 7–18% for single magnetic treatment. Similar trends were reported in [26], where combined magnetic-vibration treatment at 50 Hz (magnetic) and 70 Hz (vibration) produced stress reductions of approximately 40% and 28% in longitudinal and transverse residual stress, respectively. Another effective hybrid approach combines a pulsed magnetic field with a pulsed current, exploiting the coupled effects of magnetoplasticity and electroplasticity. Cai and Huang [9] found that pulsed magnetic treatment alone reduced stress by about 10% and pulsed current alone increased stress by approximately 20%, whereas the combined treatment produced a net stress reduction of roughly 60%. Ashi et al. [27] studied the alternating magnetic-electric treatment of machined thin-walled 7050 aluminum alloy parts; they reported residual stress reductions up to 0.85% using 50 Hz alternating fields. Thermomagnetic treatment has also demonstrated effectiveness in previous studies [28].

The underlying mechanisms of electromagnetic stress relief have been studied through several models. In 1965, Chebotkevich first proposed the phenomenon of magnetoplasticity, showing that static and low-frequency alternating magnetic fields can influence dislocation motion and macroscopic plasticity in ferromagnetic materials [29]. Since then, it has been recognized that electromagnetic fields can alter a wide range of microstructural features and properties, including grain size, phase transformation, dislocation density, texture evolution, strain distribution, atomic diffusion, recrystallization, tensile strength, fatigue performance, wear resistance, corrosion resistance, and the residual-stress state. Xie et al. [29] provided a comprehensive review of these effects, outlining possible interaction mechanisms—both thermal and athermal—between electromagnetic fields and metallic materials.

Despite these advances, most studies on alternating magnetic stress relief have employed low excitation frequencies. High-frequency alternating magnetic fields introduce a different set of physical phenomena. In conductive metals, increasing the frequency produces a pronounced skin effect: induced eddy currents concentrate near the surface, reducing penetration depth and intensifying surface heating. The skin depth decreases with frequency according to the material's resistivity and magnetic permeability. This non-uniform current distribution limits field penetration into the specimen interior and alters the spatial distribution of induced thermal and mechanical effects. In addition, the induced eddy currents oppose the applied field, which can reduce the effective magnetic field within the conductor and, consequently, the magnitude of induced mechanical stresses. At the same time, when the excitation frequency approaches a component's natural frequency, the specimen can experience large-amplitude resonance, generating higher mechanical stresses and promoting more efficient energy transfer into the material. Therefore, high-frequency alternating magnetic treatment is not simply a scaled-up version of low-frequency excitation; its effectiveness depends on the balance among electromagnetic penetration, surface heating, eddy-current shielding, and resonance-induced vibration. This complexity is one reason why high-frequency alternating magnetic stress relief remains less explored than pulsed or low-frequency alternating methods.

Although earlier studies demonstrated that low-frequency alternating magnetic fields can reduce residual stress in welded specimens, there is limited experimental evidence on high-frequency alternating excitation tuned near structural natural frequencies, particularly for welded ferritic stainless-steel components. The present study addresses this gap by investigating high-frequency alternating magnetic excitation near the natural frequencies of welded 430 steel.

Accurate residual stress measurement is essential for evaluating stress relief techniques. Available methods are either destructive (e.g., hole-drilling) or non-destructive (e.g., X-ray diffraction, ultrasonic testing). Nanoindentation is a localized, non-destructive technique capable of quantifying residual stresses by analyzing force-displacement curves, which are sensitive to stress magnitude and type (tensile/compressive) [30–33]. Pioneering work by Stone et al. [34] first demonstrated residual stress measurement in aluminum films via nanoindentation. Subsequent studies by Tsui et al. [35] on aluminum alloys established correlations between indentation behavior and applied stress states. Suresh and Giannakopoulos [36] developed foundational models for residual stress estimation using sharp indenters, while Carlson and Larson [37] derived relationships between hardness, residual strain, and contact area in steel. More recently, Wang et al. [38] proposed an energy-based method for calculating compressive stress, validated via finite element analysis. Ghanbari and Baher [39] extended this approach to tensile stresses using the energy method. Experimental validation by Greco et al. [40] confirmed strong agreement between nanoindentation and X-ray diffraction measurements, reinforcing the reliability of nanoindentation for residual stress assessment.

Although previous research has investigated various magnetic stress relief methods, including pulsed and low-frequency alternating fields, applied to different materials, and nanoindentation has been utilized for residual stress measurement in various contexts, there is limited research focusing on the application of high-frequency alternating magnetic fields, particularly those tuned to a component's natural frequencies, for residual stress relief in welded 430 steel.

This study experimentally investigates the effectiveness of high-frequency alternating magnetic field treatment, with excitation frequencies tuned near the material's natural frequencies, for reducing residual stresses induced by laser welding in 430 steel. Laser welding is chosen for its precision and uniformity in inducing residual stress in specimens. 430 steel is selected due to its ferritic structure and strong magnetic properties, making it responsive to magnetic treatment. Nanoindentation is employed to quantify the residual stress before and after the treatment.

The paper is structured as follows: Section 2 details the experimental methods, Section 3 presents the nanoindentation results, Section 4 discusses the residual stress calculation and analysis, and Section 5 provides conclusions based on the observed stress relief.

2. Experimental Methods

In this research, the release of the residual stresses included by the welding process using a variable magnetic field is studied experimentally. Based on the analyses and simulations reported in previous studies [41, 42], it has been found that the greatest residual stresses generated during the welding process are both longitudinal and perpendicular to the weld line. These stresses are approximately half of the yield stress of the material. Consequently, the induced stresses should also be around half of the yield stress to facilitate the release of residual stress at room temperature. An experimental study conducted by Farhadi and Aslani [43] demonstrated that alternating magnetic fields generated by a high-frequency square signal in a small U-shaped coil can excite steel specimens near their resonance frequencies or the corresponding subharmonics. This phenomenon results in relatively large amplitude stresses in the steel components.

Components made of 430 steel, which possesses relatively strong magnetic properties, were utilized in this study. The specimens were cut from a rolled steel sheet with a thickness of 2 mm, a width of 25 mm, and a length of 240 mm using laser cutting. The size of the components was selected so that their natural frequencies would fall within a range that could be easily excited into resonance using the available equipment. Before testing, the specimens were annealed to relieve the initial residual stresses and those induced by the laser-cutting process. All parts were placed in an oven at

800 °C for 20 minutes.

To induce the required residual stress in the specimens, laser welding was used. The reason for choosing this welding technique was its precision and uniformity along the weld line. In this study, the diameter of the filler wire was 0.8 mm, and the amperage of the device was set at 40 A. A total of six welding lines were performed on each specimen to induce significant residual stress. As illustrated in Fig. 1, the parts were bent by approximately 10 degrees due to the residual stress generated during the welding process. The consistent bending of approximately 10° observed across all welded specimens (Fig. 1) provided a preliminary visual confirmation that the multi-pass welding procedure had been applied uniformly, ensuring a comparable initial residual stress state in all specimens prior to magnetic treatment.

A U-shaped coil with a ferrite core placed in direct contact with the steel strips was utilized to perform the stress relief treatment (see Fig. 2). The core geometry was designed to maximize the coupling of the magnetic flux with the specimen. The core width (15 mm) was selected according to the specimen width (to concentrate the flux over the fusion zone and heat-affected zone rather than the entire specimen width), and the leg spacing was set to span the fusion zone with adequate clearance for positioning and to directly affect the heat-affected zone. The core cross-section was selected to avoid magnetic saturation at the expected field strengths, and ferrite was chosen as the core material for its high permeability and low losses in the kHz frequency range. Direct contact between the core legs and the specimen surface ensured efficient flux transfer during treatment.
The coil was wrapped with 0.45 mm diameter copper wire, which formed 200 turns around the core. A finite element model of the specimen was prepared in COMSOL to determine the natural frequencies of the part. The FEM results showed that the first and second natural frequencies were 6100 Hz and 12,200 Hz, respectively.

The COMSOL model was used solely to estimate the natural frequencies of the stress-free annealed specimen geometry. Although the welding process introduces

Fig. 1. Bending of specimens due to residual stress induced by welding.

metallurgical changes and measurable distortion in the specimen (approximately 10° of bending, as shown in Fig. 1), we assumed that the resulting shifts in the longitudinal natural frequencies remain modest. The natural frequencies of longitudinal vibration depend primarily on Young's modulus, material density, mass distribution, and geometry of the component. While welding can alter each of these properties to some degree -through microstructural evolution, the introduction of residual stresses, and geometric distortion- the net effect on the lower natural frequencies is generally limited. This is because these frequencies are governed by global structural characteristics rather than localized changes near the weld zone. To further account for possible frequency shifts, the excitation was applied at the calculated natural frequencies as well as several auxiliary excitation frequencies (e.g., 1000 Hz, which is close to the 1/6 subharmonic: 6100/6 ≈ 1017 Hz), ensuring that effective coupling could be achieved even if the actual resonant frequencies deviated slightly from the predicted values.

To apply the desired excitation to the coil and induce the necessary stress in the specimens, a sinusoidal signal at the appropriate excitation frequency was fed into a Lab Gruppen PDX3000 amplifier for amplification. As recommended by the device manufacturer, a small electrical resistor capable of withstanding high currents was placed in the amplifier's output circuit to limit the current and protect the instrument from potential damage during operation. To meet the manufacturer's specification while accommodating the expected current

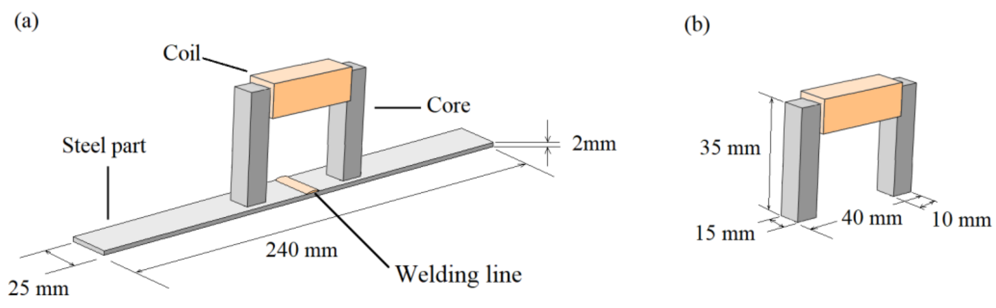

Fig. 2. The configuration and designed dimensions of the welded specimen and the coil for the stress relief test. The coil makes direct contact with the central area of the steel specimen.

levels, several parallel resistors were connected, providing a total resistance of 8.7 Ω and a power rating of several hundred watts. In addition to its protective function, the known resistance value enabled the calculation of the coil current from the measured voltage drop, as reported in Table 1.

Experimental results (Ref. [43]) have demonstrated that as the excitation frequency increases, the equivalent electrical impedance of the excitation circuit rises sharply. Consequently, the induced magnetic field gradually diminishes at a fixed voltage. On the other hand, as the frequency approaches the component's natural frequency, excitation becomes easier to achieve even with smaller induced forces. Additionally, due to the nonlinear dynamics of the system (encompassing mechanical, electrical, and magnetic interactions), the frequency of the applied magnetic force contains components at the excitation frequency and its integer harmonics. These factors make the selection of an optimal frequency for maximizing vibration and, thereby, stress relief- somewhat case-dependent and challenging. To ensure the application of the maximum induced stress, this study adopts the component’s natural frequency and several of its approximate subharmonics as the excitation frequencies.

In this treatment, a variable magnetic field was applied to the specimens using a sinusoidal current with a frequency of 6100 Hz for 30 seconds. This procedure was then repeated with a sinusoidal signal at 12200 Hz, a sinusoidal signal at 1000 Hz, and a square wave at 1000 Hz. A 60-second interval was maintained between the different excitations.

The selection of excitation frequencies was guided by the spatial distribution of residual stresses resulting from the multi-pass welding process. Because six parallel weld lines were applied to each specimen, the heat-affected zone extended across a considerable portion of the strip width, producing a likely M-shaped residual stress profile. The first natural frequency (6100 Hz) was selected because its mode shape induces large mechanical stresses in the central region of the specimen, near the fusion zone. The second natural frequency (12200 Hz) was chosen because it generates higher longitudinal stresses in the surrounding area, corresponding to the heat-affected zone. By applying both frequencies in sequence, a broad region of the specimen could be effectively stimulated.

Table 1. Specifications of the treatment procedure

Excitation parameters	Excitation frequency			
	6100 Hz (Sin)	12200 Hz (Sin)	1000 Hz (Sin)	1000 Hz (Sq)
Resistor Voltage (V)	9.7	4.8	38	48
Current (A)	1.11	0.55	4.36	5.51
Treatment time (s)	30	30	30	30
Rest time (s)	60	60	60	60

The 1000 Hz frequency was employed as an auxiliary excitation close to the 1/6 subharmonic (6100/6 ≈ 1017 Hz). As discussed by Farhadi and Aslani [43], nonlinear coupling among the mechanical, electrical, and magnetic subsystems can generate responses at integer harmonics and subharmonics of the driving frequency, thereby broadening the frequency content of the excitation. The 1000 Hz signal was applied in both sinusoidal and square-wave forms to allow a direct comparison of the two waveforms under similar conditions.

Each frequency was applied for 30 seconds. This duration was found to provide sufficient time for stress relaxation through dislocation motion while limiting resistive heating of the coil and the specimen. A 60-second rest interval was maintained between successive treatment steps to allow thermal dissipation and ensure that each step began from a stable temperature, thereby preventing cumulative overheating.

After the treatment, the wire-cut method was used to cut the samples for the nanoindentation test. This method introduces the least mechanical and thermal stress into the samples. As shown in Fig. 3, three circles with a diameter of 11 mm were cut from each specimen near the welding line. The centers of the samples were located at distances of 13 mm, 26 mm, and 39 mm from the welding line, respectively. In this figure, the samples taken from each specimen are labeled 1–3, corresponding to their distances from the welding line. Additionally, a sample was taken from the annealed sheet, which exhibited no residual stress.

For the nanoindentation measurements, we utilized a Digital Instruments NanoScope III device equipped with a four-sided pyramid-shaped indenter with a tip angle of approximately 156°. The procedure for the indentation test involved gradually increasing the force from zero to 5000 μN for 30 seconds. Following a 10-second pause, the unloading phase was performed over another 30 seconds. On each circular sample, the probe was applied three times at intervals of 2 μm on the upper surface (welded surface) of the samples, and force-displacement curves were recorded. Finally, by averaging the experimental data from each sample, we extracted the average force-displacement curve for that sample.

Fig. 4 illustrates the principle underlying residual stress measurement by nanoindentation and the manner in which residual stresses alter the force-displacement response. When a specimen contains compressive residual stresses, a greater force is required to drive the indenter to a given depth compared to the stress-free condition, resulting in an upward shift of the force-displacement curve. Conversely, tensile residual stresses facilitate indenter penetration, causing a downward shift relative to the stress-free reference. In the energy method employed here, the areas under the loading curves for the stress-free specimen and the specimen containing tensile residual stress are compared. The work difference between these two curves is attributed to the contribution of the residual stress field. In this figure, P_{max}^{c}, P_{max}^{s-f} and P_{max}^{t} denote the maximum force for the specimen with compressive residual stress, the stress-free specimen, and the specimen with tensile residual stress, respectively.

To estimate the residual stress induced by the welding process from the force-displacement data of the nanoindentation tests, we used the energy method presented by Ghanbari and Baher [39]. To explain the method, the force-displacement curves presented in Fig. 4 can be used. They assumed that the work of elastic stresses is negligible compared to the work done by plastic stresses, and therefore, the work of plastic forces can be estimated as follows:

$$U_{pl} \approx U_{el+pl} = \int_0^{h_{max}} P(h)dh. \quad P(h) = \beta h^m, \quad (1)$$

Where $P(h)$ is the penetration force at the penetration depth h, h_{max} is the maximum penetration depth, β is a

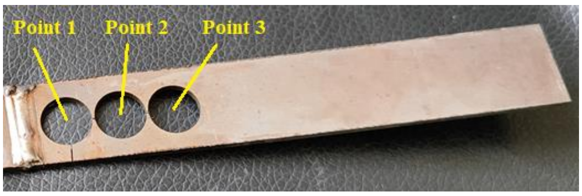

Fig. 3. Specimen preparation via wire-cut, showing sampling locations relative to the weld line. Three 11 mm-diameter circular specimens were extracted from each welded specimen at progressively increasing distances from the weld line: 13 mm (Point 1, closest), 26 mm (Point 2, intermediate), and 39 mm (Point 3, farthest).

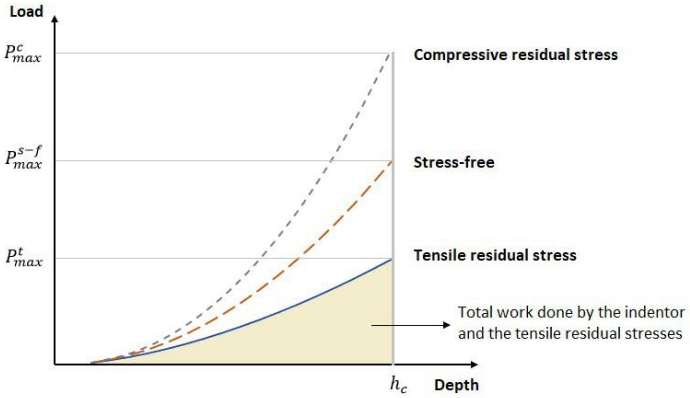

Fig. 4. Force-displacement diagram resulting from nanoindentation test for samples with and without residual stress.

constant depending on the material, and m is a constant depending on the shape of the indenter. On the other hand, the work done by plastic stresses includes the work of the stresses applied by the indenter and the tensile or compressive residual stresses. Therefore, to obtain the work of residual stresses, it is enough to subtract the force-displacement curves for samples with and without residual stress at the same penetration depth:

$$\text{Work done by tensile residual stresses} = U^{s}_{pl} - U^{s-f}_{pl} \approx \frac{P^{t}_{max}\, h_{max}}{1+m_t} - \frac{P^{s-f}_{max}\, h_{max}}{1+m_{s-f}} \quad (2)$$

In the above equation, m_{s-f} denotes the power-law exponent for the stress-free (annealed) specimen, while m_t denotes the corresponding value for the specimen with tensile residual stress.

Also, according to the analysis presented in Reference [37], the work of residual tensile stresses between the same two limits can be approximated by the following relationship:

$$\text{Work done by tensile residual stresses} = -\sigma_{res}\left(\frac{2}{3}\,\pi\, h^{2}_{max}\, tan^{2}(\alpha)\right)h_{max} \quad (3)$$

Where α is half of the indenter tip angle. Therefore, by comparing Eqs. (2) and (3), the residual stress is obtained with the following approximate relation:

$$\sigma_{res} = \frac{U^{s}_{pl} - U^{s-f}_{pl}}{\frac{2}{3}\,\pi\, h^{2}_{max}\, tan^{2}(\alpha)} = \frac{1}{\frac{2}{3}\,\pi\, h^{2}_{max}\, tan^{2}(\alpha)}\left(\frac{P^{s-f}_{max}}{m_{s-f}+1} - \frac{P^{t}_{max}}{m_t+1}\right) \quad (4)$$

3. Nanoindentation Results

As mentioned in the previous section, sinusoidal and square currents with varying frequencies were induced in the coil circuit for the stress relief treatment. Due to power limitations, as well as the voltage and current constraints of the sound card and amplifier, along with the electrical resistance and inductance of the circuit components (including the sound card, amplifier, and coil circuit), the current and output voltage characteristics depend on the excitation frequency. Table 1 displays the treatment specifications, including the excitation frequency, resistor voltage (connected in series with the coil), circuit current, treatment step duration, and the rest time between treatment steps.

The indentation tests were conducted on the surfaces of the specimens where the welding operation occurred. It is known that the residual stress on these surfaces is tensile. Furthermore, this tensile residual stress reduces the slope of the force-displacement curve, as shown in Fig. 4. Consequently, after the electromagnetic treatment, we expect a reduction in the residual stresses, which will lead to an increase in the slope of the curve. As a result, the diagram for the treated area is anticipated to tilt slightly to the left compared to its previous state.

Fig. 5 illustrates the force-displacement curves obtained from different specimens. The plotted curves for each measurement point represent averaged force-displacement data obtained from multiple tests at that specific location. According to the figure, in all samples, the force - displacement graphs shift to the left as the distance from the welding line increases. This shift indicates a decrease in tensile residual stress. In addition, the force-displacement diagrams for the treated components remain comparable, despite some differences. This suggests relatively uniform changes in residual stress at similar locations within the treated specimens.

Fig. 6 compares the force-displacement curves of the virgin specimen with those of the control specimen and the stress-relieved specimen at various distances from the weld line. The figure illustrates that the treatment has a significant impact on the treated parts. Compared to the untreated specimen, the curves for the treated specimens have shifted to the left, aligning more closely with the curve of the virgin specimen at all three measured distances from the weld line. This shift indicates a considerable reduction in tensile residual stress in the treated specimens.

4. Calculation of Residual Stress

Eq. (4) has been employed to measure the residual stress. To utilize this relationship effectively, it is necessary to estimate the exponent of the exponential expression in Eq. (1) appropriately. In most cases, fitting the best power curve using the least squares method yields satisfactory results; however, some curves exhibit non-negligible deviations. Consequently, to determine the work done by the indenter, the area under the force-displacement curve has been calculated directly using the numerical (trapezoidal) integration method. Table 2 presents the estimated residual stresses before and after the stress relief operation. It is important to note that the yield stress of 430 steel is 345 MPa, and the ultimate tensile strength of this material is 517 MPa [44]. At point 1, the residual stress has decreased by approximately 38% compared to the control specimen. At points 2 and 3, the reductions in residual stress are 80% and 84%, respectively. These results demonstrate that, despite utilizing relatively simple and inexpensive equipment, the method of high-frequency magnetic stress relief is highly effective in reducing residual stresses.

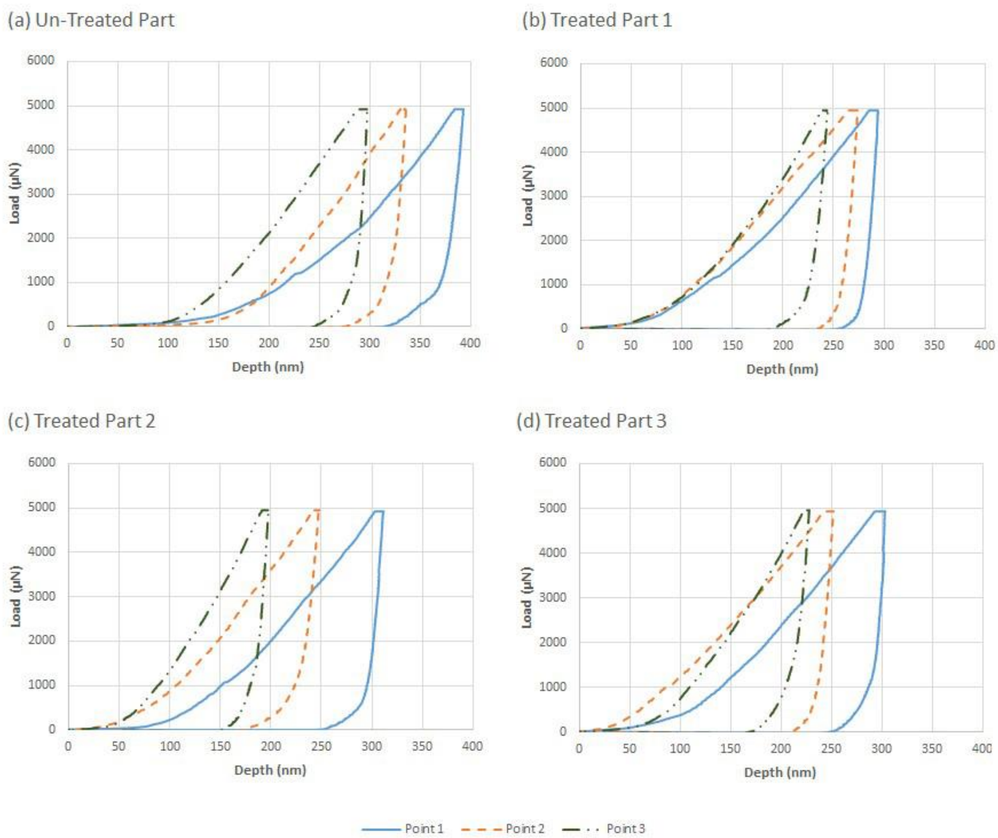

Fig. 5. Nanoindentation force-displacement curves for different specimen conditions: (a) as-welded (untreated), (b) magnetically treated sample 1, (c) magnetically treated sample 2, and (d) magnetically treated sample 3. Each curve represents the averaged response from multiple indentation tests at each measurement point.

Table 2. The results of the electromagnetic stress relief operation

Measurement results	Sampling points		
	Point 1	Point 2	Point 3
Residual stress (MPa)- Untreated part	220.14	224.63	149.16
Residual stress (MPa)- Treated parts (Avg.)	134.72	45.09	24.36
Relaxed Stress (MPa)	85.42	179.54	124.8
Relaxed Stress (%)	38	80	84

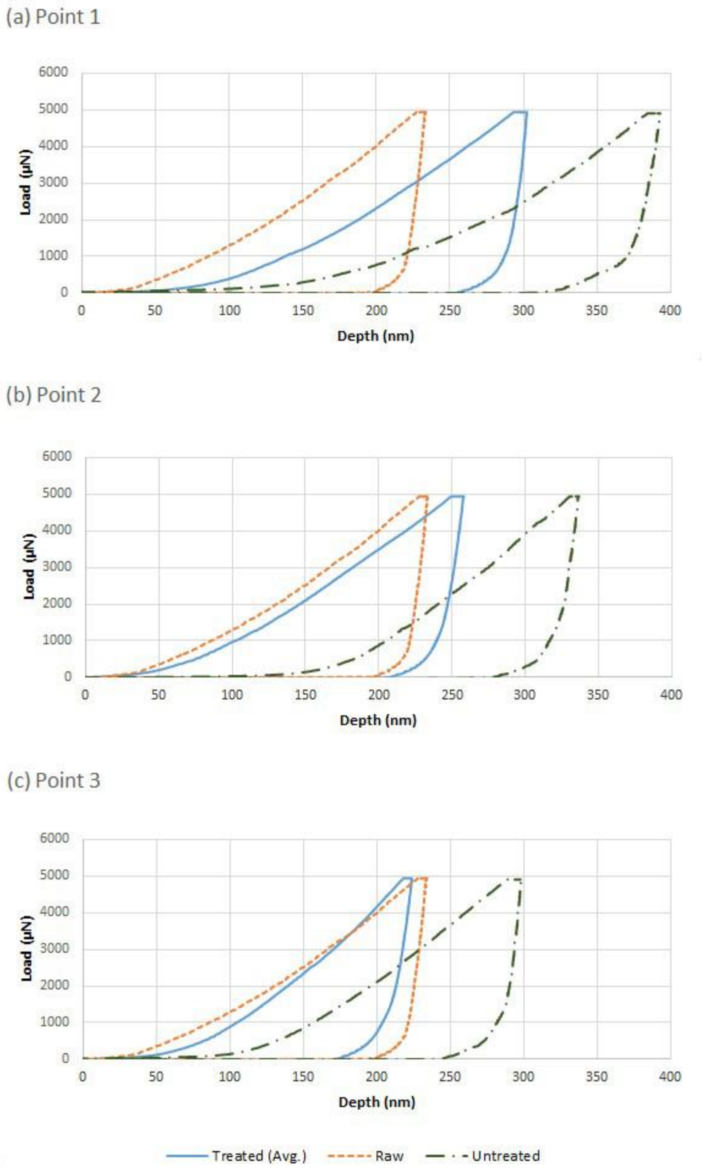

Fig. 6. Comparison of the overall averaged force-displacement curves for treated specimens with the untreated and virgin specimens at various distances from the welding line. The results for the stress-relieved samples were obtained by averaging corresponding samples from all specimens.

It is worth commenting on the spatial distribution of residual stress before and after treatment. In the untreated specimen, the residual stress values at Points 1 (220.14 MPa), 2 (224.63 MPa), and 3 (149.16 MPa) suggest an M-shaped profile across the width of the strip. This shape is consistent with the multi-pass welding procedure employed in this study, where six parallel weld lines create overlapping thermal cycles and heat-affected zones. Under these conditions, the peak tensile residual stress can shift from the weld centerline to the adjacent heat-affected zone, producing local maxima on either side of the fusion zone rather than a single central peak. After magnetic treatment, the average residual stresses at the same locations were reduced to 134.72 MPa, 45.09 MPa, and 24.36 MPa, respectively, indicating that the M-shaped distribution was substantially flattened. The most pronounced relaxation occurred in the intermediate and far-field regions, where the induced vibratory stresses from the second natural frequency mode (12200 Hz) are expected to be most effective.

The untreated near-weld residual stress measured in this study (approximately 220 MPa) falls within the expected range for welded steel plates, which is typically reported to be around half the material's yield stress [41]. For 430 steel (yield stress of 345 MPa), this corresponds to roughly 170–200 MPa, confirming that our measurements are physically reasonable. Furthermore, Greco et al. [40] demonstrated strong agreement between nanoindentation-based residual stress measurements and X-ray diffraction, supporting the reliability of the energy method employed here. It should also be noted that the principal aim of this study was to compare residual stress levels before and after treatment, and at different distances from the weld line, using identical measurement and analysis procedures throughout. Under these conditions, the comparative trends—namely, the progressive increase in stress relaxation from 38% near the centerline to 84% in the far field—are robust and do not depend on the absolute numerical precision of the method.

It is worth noting that the present experiments were conducted under the voltage and current constraints of the available amplifier and coil circuit (see Table 1). Without these limitations, higher magnetic field intensities could be applied, which would likely produce greater induced stresses and potentially more complete stress relief, particularly in the near-weld region where the current treatment achieved a 38% reduction. However, operating at substantially higher power levels would introduce additional considerations, including the risk of excessive resistive heating, the possible onset of nonlinear magnetomechanical behavior, and the potential to inadvertently introduce new residual stresses. Optimizing the balance between field intensity, treatment duration, and thermal management remains an area for future investigation.

Efforts were made to numerically simulate the magnetic stress induction process in COMSOL—that is, the mechanical stresses generated in the specimen by the applied alternating magnetic field under the same excitation parameters used experimentally. However, the strongly coupled electromagnetic–mechanical nature of the problem, combined with nonlinear magnetostrictive effects and the complex resonance dynamics at kHz frequencies, prevented quantitative agreement with simulations and the experimental observations. While the simulations captured the general trends, reliable numerical prediction of the induced stress field remains a challenge that warrants further investigation. Direct experimental validation of the nanoindentation-derived residual stresses using complementary techniques such as X-ray diffraction or hole-drilling is also recommended for future studies.

5. Conclusion

This research investigated the effectiveness of high-frequency alternating magnetic field treatment for relieving residual stresses induced by multi-pass laser welding in 430 ferritic stainless steel. The treatment employed excitation frequencies tuned to the component's first and second natural frequencies (6100 Hz and 12200 Hz), supplemented by approximate subharmonic excitation at 1000 Hz (6100/6 ≈ 1017 Hz) to broaden the frequency response through nonlinear coupling. The core geometry was designed to concentrate magnetic flux over the fusion zone and heat-affected zone, and direct core-to-specimen contact ensured efficient flux transfer. Residual stresses were assessed before and after treatment using the nanoindentation energy method on specimens extracted at three distances from the weld line. The key findings of this study are as follows:

1. **Significant stress relief was achieved across all measurement locations.** The alternating magnetic treatment reduced residual stresses by 38% near the weld line (Point 1, 13 mm), 80% at the intermediate location (Point 2, 26 mm), and 84% in the far-field

region (Point 3, 39 mm). These results demonstrate that high-frequency magnetic stress relief is highly effective despite utilizing relatively simple and inexpensive equipment.

2. **Treatment effectiveness increased with distance from the weld line.** The stress relaxation percentage rose progressively from 38% at the nearest measurement point to 84% at the farthest. This trend suggests that the combined application of the first and second natural frequency modes—which respectively target the central fusion zone and the surrounding heat-affected zone—successfully stimulated a broad area, with the most complete relaxation occurring in regions where the initial residual stress magnitude was moderate.
3. **The residual stress distribution in the untreated specimen exhibited an M-shaped profile.** The slightly higher residual stress at Point 2 compared to Point 1 is attributed to the multi-pass welding procedure, in which overlapping thermal cycles from six parallel weld lines expand the heat-affected zone and displace the peak tensile stress away from the weld centerline. After magnetic treatment, this M-shaped distribution was substantially flattened, indicating effective stress relief across the entire affected region.
4. **The nanoindentation energy method provided a consistent basis for comparative residual stress assessment.** Although direct experimental validation using complementary techniques such as X-ray diffraction was not performed in this study, the measured near-weld residual stress (approximately 220 MPa) is consistent with the expected range for welded steel plates, and the comparative trends are robust given that all measurements were performed under identical conditions.

Overall, the study found that the alternating magnetic field method is an effective approach for relieving residual stress in welded steel components. It is a relatively simple and efficient technique that can enhance the performance and lifespan of welded components.

Further research is recommended to fine-tune the various factors that influence the efficiency of this method. Exploring the effects of magnetic field frequency, intensity, and treatment duration could provide valuable insights. Numerical simulation of the magnetic stress induction process, which was attempted in parallel with this work but did not yield quantitatively comparable results due to the complex coupled physics involved, remains an important challenge for future investigation. Additionally, this method could be applied to relieve residual stress in other materials and welded geometries, and direct experimental validation using complementary measurement techniques would further strengthen confidence in the findings reported here.

Author’s contributions

P. Mardookh Rohani: Experiments, Investigation, Formal analysis, Software, Validation, Visualization, Writing - original draft

S. Farhadi: Conceptualization, Methodology, Supervision, Software, Resources, Validation, Formal analysis, Visualization, Writing - original draft, Review & editing

A. Hasani: Methodology, Review & editing

Competing interests

The authors have no competing interests to declare.

Funding

This research received no specific grant from any funding agency in the public, commercial, or not-for-profit sectors.

Data availability

The raw data required to reproduce the above findings are available to download from [https://drive.google.com/file/d/1mDmb2b57-OAA1ob9qPyV0WOQyl5CHoil/view?usp=drive_link].

6. References

[1] Nasir, N. S., Razab, M. K., Mamat, S., & Iqbal, M. (2016). Review on welding residual stress. *ARPN Journal of Engineering and Applied Sciences*, *11*(9), 6166-6175.

[2] Liu, Q., Wang, C., Shang, C., & Li, J. (2025). Design of a multi-manipulator robot for relieving welding residual stress. *Industrial Robot: The International Journal of Robotics Research and Application*, *52*(2), 183-194. https://doi.org/10.1108/IR-05-2024-0219

[3] Kannatey-Asibu J, E. (2009). *Principles of laser materials processing*. John Wiley & Sons. https://doi.org/10.1002/9780470459300

[4] Huang, G., Zhou, C., Liu, R., & Hu, S. (2024). An investigation into the reduction mechanism of temperature-magnetic stress relief based on DO3 crystal. *Results in Physics*, *60*, 107644. https://doi.org/10.1016/j.rinp.2024.107644

[5] Wang, J. S., Hsieh, C. C., Lin, C. M., Chen, E. C., Kuo, C. W., & Wu, W. (2014). The effect of residual stress relaxation by the vibratory stress relief technique on the textures of grains in AA 6061 aluminum alloy. *Materials Science and Engineering: A*, *605*, 98-107. https://doi.org/10.1016/j.msea.2014.03.037

[6] Ashi, L., Xie, Z., Sun, H., Wang, J., & Huang, K. (2023). Effect of electromagnetic coupling treatment on the residual stress relief and mechanical properties of 7050 aluminum alloy. *Journal of Materials Science*, *58*(29), 12097-12117. https://doi.org/10.1007/s10853-023-08775-y

[7] Lu, A. L., Tang, F., Luo, X. J., Mei, J. F., & Fang, H. Z. (1998). Research on residual-stress reduction by strong pulsed magnetic treatment. *Journal of Materials Processing Technology*, *74*(1-3), 259-262. https://doi.org/10.1016/S0924-0136(97)00280-X

[8] Shao, Q., Kang, J., Xing, Z., Wang, H., Huang, Y., Ma, G., & Liu, H. (2019). Effect of pulsed magnetic field treatment on the residual stress of 20Cr2Ni4A steel. *Journal of Magnetism and Magnetic Materials*, *476*, 218-224. https://doi.org/10.1016/j.jmmm.2018.12.105

[9] Cai, Z., & Huang, X. (2011). Residual stress reduction by combined treatment of pulsed magnetic field and pulsed current. *Materials Science and Engineering: A*, *528*(19-20), 6287-6292. https://doi.org/10.1016/j.msea.2011.04.078

[10] Cai, Z. P., Lin, J. A., Zhou, L. A., & Zhao, H. Y. (2004). Evaluation of effect of magnetostriction on residual stress relief by pulsed magnetic treatment. *Materials Science and Technology*, *20*(12), 1563-1566. https://doi.org/10.1179/026708304X4286

[11] Li, X., Tang, Y., Zhang, Y., Liu, H., Cao, Q., Lai, Z., Han, X., & Li, L. (2022). Relaxation of the residual stress in an aluminum alloy ring by electromagnetic bulging methods. *IEEE Transactions on Applied Superconductivity*, *32*(6), 1-5. https://doi.org/10.1109/TASC.2022.3149728

[12] Shao, Q., Wang, G., Wang, H., Xing, Z., Fang, C., & Cao, Q. (2021). Improvement in uniformity of alloy steel by pulsed magnetic field treatment. *Materials Science and Engineering: A*, *799*, 140143. https://doi.org/10.1016/j.msea.2020.140143

[13] Hou, M., Li, K., Li, X., Zhang, X., Rui, S., Wu, Y., & Cai, Z. (2020). Effects of pulsed magnetic fields of different intensities on dislocation density, residual stress, and hardness of Cr4Mo4V steel. *Crystals*, *10*(2), 115. https://doi.org/10.3390/cryst10020115

[14] Yan, M., Wang, C., Luo, T., Li, Y., Feng, X., Huang, Q., & Yang, Y. (2021). Effect of pulsed magnetic field on the residual stress of rolled magnesium alloy AZ31 sheet. *Acta Metallurgica Sinica (English Letters)*, *34*, 45-53. https://doi.org/10.1007/s40195-020-01109-w

[15] Zhong, F., Wang, J., Zhang, Q., Huang, J., Wang, W., Xu, J., Huang, K., & Qin, Y. (2022). Residual stress reductions of carbide cutting tools through applying pulsed magnetic field and coupled electromagnetic field. *The International Journal of Advanced Manufacturing Technology*, *121*(7), 4757-4775. https://doi.org/10.1007/s00170-022-09434-3

[16] Wang, Y., Xing, Z., Huang, Y., Guo, W., Kang, J., Wang, H., & Zhang, Z. (2021). Effect of pulse magnetic field treatment on the hardness of 20Cr2Ni4A steel. *Journal of Magnetism and Magnetic Materials*, *538*, 168248. https://doi.org/10.1016/j.jmmm.2021.168248

[17] Fahmy, Y., Hare, T., Tooke, R., & Conrad, H. (1998). Effects of a pulsed magnetic treatment on the fatigue of low carbon steel. *Scripta Materialia*, *38*(9), 1355-1358. https://doi.org/10.1016/S1359-6462(98)00046-3

[18] Zhang, Y., Fang, C., Huang, Y., Guo, W., Xing, Z., Wang, H., & Zhang, Z. (2021). Enhancement of fatigue performance of 20Cr2Ni4A gear steel treated by pulsed magnetic treatment. *Journal of Magnetism and Magnetic Materials*, *540*, 168327. https://doi.org/10.1016/j.jmmm.2021.168327Get rights and content

[19] Tang, G., Xu, Z., Tang, M., Chen, X., Zhou, H., & Lu, A. (2005). Effect of a pulsed magnetic treatment on the dislocation substructure of a commercial high strength steel. *Materials Science and Engineering: A*, *398*(1-2), 108-112. https://doi.org/10.1016/j.msea.2005.03.003

[20] Li, X., Tang, X., Li, M., Liu, Q., Tuo, Z., Cao, Q., & Li, L. (2025). Relaxation of residual stress in aluminum alloy rings by pulsed high magnetic field. *Journal of Materials Processing Technology*, *338*, 118778. https://doi.org/10.1016/j.jmatprotec.2025.118778

[21] Tang, F., Lu, A. L., Mei, J. F., Fang, H. Z., & Luo, X. J. (1998). Research on residual stress reduction by a low frequency alternating magnetic field. *Journal of Materials Processing Technology*, *74*(1-3), 255-258. https://doi.org/10.1016/S0924-0136(97)00279-3

[22] Wu, S., Lu, A., Zhao, H., Fang, H., & Tang, F. (2002). Micromechanism of residual stress reduction by low

frequency alternating magnetic field treatment. *Materials Science and Engineering: A, 328*(1-2), 133-136. https://doi.org/10.1016/S0921-5093(01)01682-3

[23] Song, Y., Hua, L., & Wang, B. (2009). Reduction of residual stress in low alloy steel with magnetic treatment in different directions. *Journal of Wuhan University of Technology- Materials Science Edition*, *24*(6), 857-862. https://doi.org/10.1007/s11595-009-6857-8

[24] Song, Y., & Hua, L. (2012). Mechanism of residual stress reduction in low alloy steel by a low frequency alternating magnetic treatment. *Journal of Materials Science & Technology*, *28*(9), 803-808. https://doi.org/10.1016/S1005-0302(12)60134-0

[25] Huang, G., & Li, B. (2023). The combined magnetic-vibration stress relief. *Results in Physics, 47*, 106372. https://doi.org/10.1016/j.rinp.2023.106372

[26] Huang, G., Liu, R., & Hu, S. (2023). Investigation of the mechanism for reduction of residual stress through magnetic-vibration stress relief treatment. *Journal of Magnetism and Magnetic Materials*, *582*, 171041. https://doi.org/10.1016/j.jmmm.2023.171041

[27] Ashi, L., Xie, Z., Sun, H., Wang, J., & Huang, K. (2023). Effect of electromagnetic coupling treatment on the residual stress relief and mechanical properties of 7050 aluminum alloy. *Journal of Materials Science*, *58*(29), 12097-12117. https://doi.org/10.1007/s10853-023-08775-y

[28] Huang, G., & Zhou, C. (2025). Thermomagnetic Treatment for Residual Stress Reduction. *Journal of Materials Engineering and Performance*, *34*(17), 18858-18864. https://doi.org/10.1007/s11665-025-10633-8

[29] Xie, L., Sun, H., Wen, Y., Hua, L., & Zhang, L. C. (2025). Electromagnetic treatment enhancing performance of metal materials: A review. *Progress in Materials Science*, *153*, 101488. https://doi.org/10.1016/j.pmatsci.2025.101488

[30] Li, X., & Bhushan, B. (2002). A review of nanoindentation continuous stiffness measurement technique and its applications. *Materials Characterization*, *48*(1), 11-36. https://doi.org/10.1016/S1044-5803(02)00192-4

[31] Hu, C., & Li, Z. (2015). A review on the mechanical properties of cement-based materials measured by nanoindentation. *Construction and Building Materials, 90*, 80-90. https://doi.org/10.1016/j.conbuildmat.2015.05.008

[32] Bushan, B. (Ed.). (2020). *Handbook of micro/nano tribology*. CRC press. https://doi.org/10.1201/9780367802523

[33] Jiang, G. U. O., Haiyang, F. U., Bo, P. A. N., & Renke, K. A. N. G. (2021). Recent progress of residual stress measurement methods: A review. *Chinese Journal of Aeronautics*, *34*(2), 54-78. https://doi.org/10.1016/j.cja.2019.10.010

[34] Stone, D., La Fontaine, W. R., Alexopoulos, P., Wu, T. W., & Li, C. Y. (1988). An investigation of hardness and adhesion of sputter-deposited aluminum on silicon by utilizing a continuous indentation test. *Journal of Materials Research*, *3*(1), 141-147. https://doi.org/10.1557/JMR.1988.0141

[35] Tsui, T. Y., Oliver, W. C., & Pharr, G. M. (1996). Influences of stress on the measurement of mechanical properties using nanoindentation: Part I. Experimental studies in an aluminum alloy. *Journal of Materials Research*, *11*(3), 752-759. https://doi.org/10.1557/JMR.1996.0091

[36] Suresh, S., & Giannakopoulos, A. E. (1998). A new method for estimating residual stresses by instrumented sharp indentation. *Acta Materialia*, *46*(16), 5755-5767. https://doi.org/10.1016/S1359-6454(98)00226-2

[37] Carlsson, S., & Larsson, P. L. (2001). On the determination of residual stress and strain fields by sharp indentation testing. *Acta Materialia*, *49*(12), 2193-2203. https://doi.org/10.1016/S1359-6454(01)00122-7

[38] Wang, Q., Ozaki, K., Ishikawa, H., Nakano, S., & Ogiso, H. (2006). Indentation method to measure the residual stress induced by ion implantation. *Nuclear Instruments and Methods in Physics Research Section B*, *242*(1-2), 88-92. https://doi.org/10.1016/j.nimb.2005.08.008

[39] Ghanbari, S., & Bahr, D. F. (2019). An energy-based nanoindentation method to assess localized residual stresses and mechanical properties on shot-peened materials. *Journal of Materials Research*, *34*(7), 1121-1129. https://doi.org/10.1557/jmr.2019.41

[40] Greco, A., Sgambitterra, E., Guagliano, M., & Furgiuele, F. (2024). Measurement of laser shock peening induced residual stress by nanoindentation and comparison with XRD technique. *Journal of Materials Research and Technology*, *30*, 5701-5710. https://doi.org/10.1016/j.jmrt.2024.05.017

[41] Majzoobi, G. H., Seifi, R., Ali-akbar, S. (2012). Experimental and numerical study of temperature distribution and determination of residual stresses due to welding of plates. *Journal of Modeling Engineering*, *9*, 49-60.

[42] Nouri, Z. (2019). Investigating the effect of magnetic volumetric forces on the release of residual stresses in welding [Master's thesis, University of Kurdistan].

[43] Farhadi, S., & Aslani, M. (2023). Stress induction in steel parts using alternating magnetic field. *Mechanic of Advanced and Smart Materials*, *3*(3), 363-379.

[44] Boyer, H. E., & Gall, T. L. (1985). *Metals handbook; desk edition*. American Society of Metals.